Supporting Information

Mechanistic Insights into Palladium(Ⅱ)-Catalyzed Carboxylation of Thiophene and Carbon Dioxide

Qingjun Zhang[1], Youguang Ma [1, 2], Aiwu Zeng *[1, 2]

1 State Key Laboratory of Chemical Engineering, School of Chemical Engineering and Technology, Tianjin University, 300350, PR China

2 Chemical Engineering Research Center, Collaborative Innovative Center of Chemical Science and Engineering (Tianjin), PR China

1. Detailed σ-metathesis mechanism of C-H activation

Figure 1 and Figure S1 show the detailed insights of the cleavage of C-H bond in thiophene via the σ-metathesis mechanism (red curve) and the correspondingly important geometry structure parameters of the reactant complex, transition state and intermediates, respectively. During the pre-activation step, the structure of the complex is distorted, so that the metal palladium Pd dissociates from one of the coordinated oxygen atoms, and the relevant distance is elongated to 3.11 Å; there is also a weak interaction between the metal palladium Pd and the thiophene ring, where the distances between palladium Pd and alpha- and beta-carbon atoms are 2.24 Å and 2.35 Å, respectively. These two interactions facilitate the transfer of proton on the thiophene ring to the acetate ligand. This pre-activation process requires 0.90 kcal/mol, which is higher than that of the CMD mechanism. The cleavage of the C-H bond is achieved by the transfer of proton to the acetate ligand through the highly ordered four-membered ring transition state TS_1', in which the proton on the thiophene ring directly attacks the carboxylate anion ligand with transition metal palladium Pd bonding atom. In the transition state TS_1', the C-H bond length is elongated from 1.08 Å to 1.38 Å, which is longer than that of the CMD mode, and the distance between the metal palladium Pd and the carbanion is gradually reduced from 2.24 Å to 2.07 Å.

2. The Interatomic Interaction Analysis for the Intermediates

To gain the deeply understanding the characteristics of this palladium-catalyzed C-H carboxylation reaction, we visually analyze the interatomic interactions in the important intermediates for the proton abstraction and CO_2 insertion steps taking the interaction region indicator (IRI) analysis method [43] performed by the Multiwfn program [44]. The standard IRI isosurface colorbar and their corresponding chemical explanations are elucidated in Figure S3.

Figure S4 presents the results of interatomic interaction analysis of each complex in different C-H bond cleavage modes. The interaction between the metal palladium and each ligand, as well as the weak hydrogen bond interaction between the proton to be broken and the coordination dissociated oxygen atom, are shown in the dotted circle in Figure S4(a) for the reactant adduct Reactant Complex_1 formed in the pre-activation process. The comparison of the interactions within structures of Reactant Complex_1 and Reactant Complex_1' reveals that the interaction between the metal palladium and

nucleophile in the former is stronger than that in the latter since the former has a wider range of interaction region. Besides, in the former, there has a weak hydrogen bond interaction between the proton to be broken and the coordinatively dissociated oxygen atom, while in the latter, there is only mutual repulsion, and no similar attraction is found. As a result of the changes in these interactions, the energy of the pre-activation step varies depending on the C-H bond cleavage mode. In transition state structures of TS_1 and TS_1' for these two different deprotonation steps, the steric effect within the six-membered ring formed by the CMD mechanism is smaller than that in the four-membered ring formed by the σ-metathesis mechanism. For the intermediates of Int_1 and Int_1' generated after the proton is broken, there is an obvious interaction between the hydrogen atom on the carboxyl group of the acetic acid molecule and the nucleophile carbanion in the intermediate Int_1, while this interaction is very weak in the latter Int_1'. Therefore, according to the IRI analysis insights, the interaction between the substrate and palladium acetate throughout the reaction process results in a difference in the activation energy barrier and the energy required to eliminate acetic acid in these two modes. Figure S5 gives the results of interatomic interaction analysis of each complex in the CO_2 insertion step. There are obvious interactions between the nucleophile carbanion and the central carbon atom in the CO_2 molecule, as well as between metal palladium and the oxygen atom in the CO_2 molecule, in the three-membered cyclic conformation arrangement or inner-sphere complex route, demonstrating the assisted activation of metal palladium in the carbanion attacking CO_2 pathway. The metal palladium Pd does not interact with CO_2 molecule in the acyclic conformation or outer-sphere complex route; instead, the interaction between the carbanion and the acetic acid structure and the CO_2 molecule aids the CO_2 activation.

3. Variations of the Interatomic Interactions during the Reactions

For the purpose of deeply understanding the characteristics of this palladium-catalyzed C-H carboxylation reaction, we visually analyze the variations in the interatomic interactions as the reaction proceeds taking the interaction region indicator (IRI) analysis method [1] performed by the Multiwfn program [2]. We take the thiophene C-H deprotonation step and the following CO_2 insertion step as examples to briefly illustrate the changes in interatomic interactions in the reaction process.

Figure S8 gives the IRI isosurface maps with some illustrative points along the IRC route of the palladium acetate-induced thiophene deprotonation via the CMD mechanism. The reactant complex is represented by the first point from left to right. According to the color distribution of the IRI isosurface, we can confirm that there is hydrogen bond formed by the H atom to be broken in the thiophene ring and the dissociated O atom in the palladium acetate, vdW interaction, and steric effect in the thiophene ring apart from the covalent interactions of chemical bonds and coordination bonds of the metal palladium Pd central atom with various ions (carboxylate anion and the carbon atom of the C-H bond to be broken on the thiophene ring). The IRI isosurface maps show that as the reaction progresses, the associated hydrogen bond noncovalent interaction and the interactions between the metal palladium Pd and the carbanion are gradually transformed into the normally O-H chemical bond and Pd-C bond

interactions, thus the IRI isosurface maps are becoming increasingly blue in the appropriately enlarged regions, whereas the original C-H bond progressively breaks, lowering the electron density in the correspondingly bonding region leading to the transition of the strong covalent interaction to the weak attraction interaction between the carbanion and the removed proton. Furthermore, as the vdW interaction region increases, so does the interaction region between the broken proton and carbanions. In general, the breaking and formation of chemical bonds during the deprotonation process can be observed immediately using this visualization method.

Figure S9 visually shows the results of changes in the interatomic interactions along the reaction of the nucleophile carbanion attacking the electrophile CO_2. The first point from left to right corresponds to the reactant complex, in which the metal palladium Pd and the carbanion interact with the oxygen and carbon atoms in the CO_2 molecule, respectively. As the reaction goes on, the C-C bond that will be formed are gradually strengthened and then elongated along the bonding direction, resulting in the accumulation of the electron density in the bonding regions, which are mainly manifested in that the color of the IRI isosurface map becomes more and more blue in the corresponding regions. Besides, the structure of the carboxylate anion is constantly adjusted to finally form a stable product. The two blue parts of the IRI isosurface show that the electrostatic attractive interaction between the metallic palladium Pd and the formed thiophenecarboxylate anion becomes stronger and stronger.

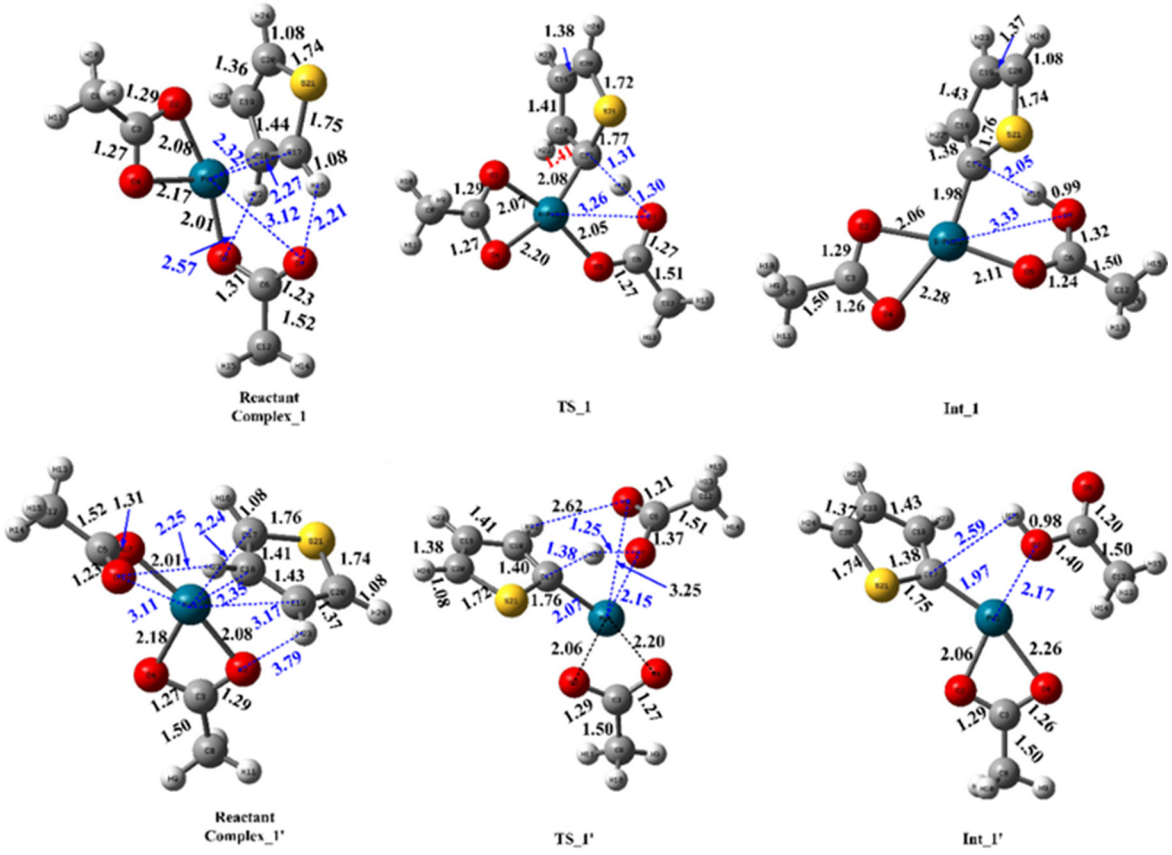

Figure S1. Structures and important geometry parameters of complexes in C-H bond cleavage step for CMD and σ-metathesis modes.

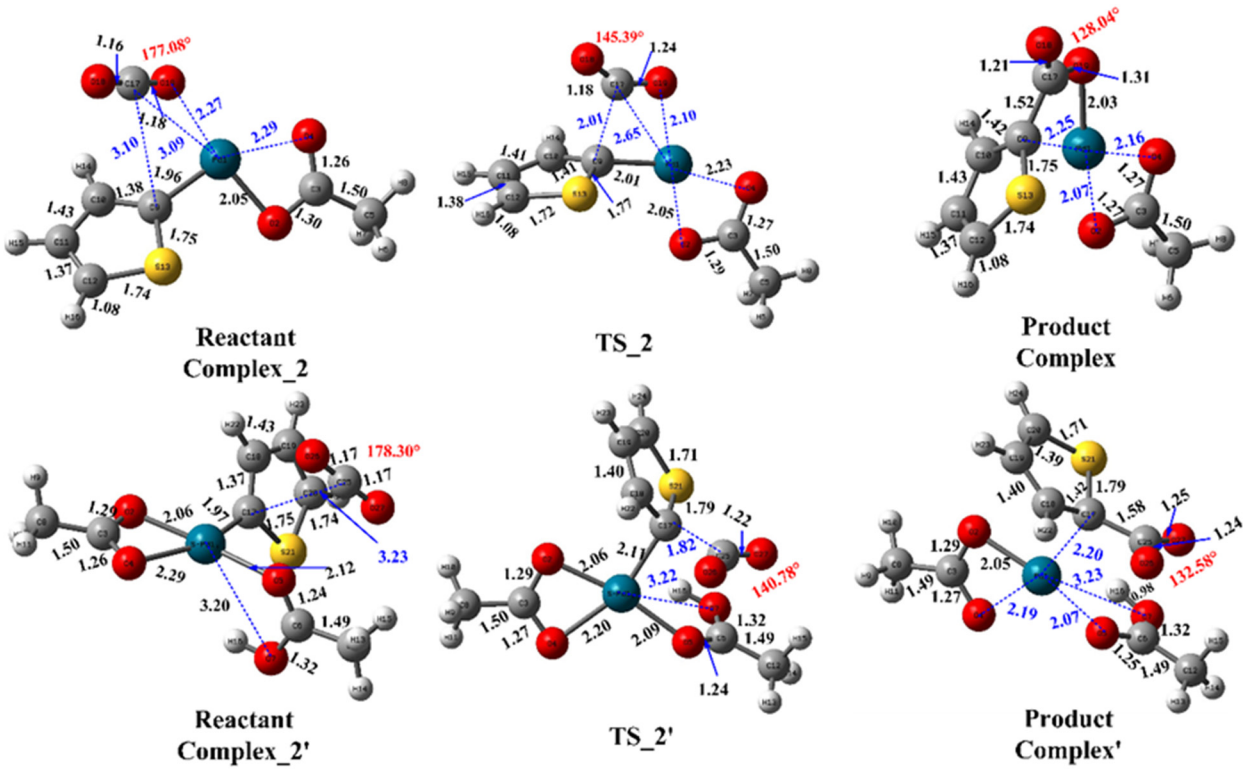

Figure S2. Structures and important geometry parameters of complexes in CO_2 insertion step.

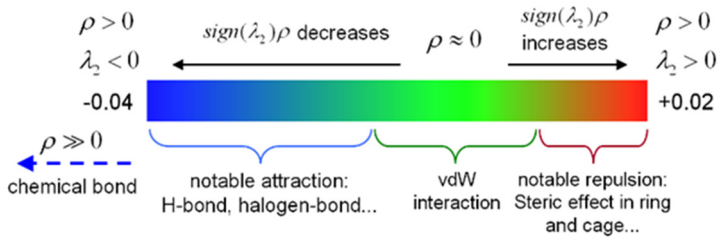

Figure S3. The standard IRI color-bar and the chemical explanations of sign(λ2)ϱ on IRI isosurface.

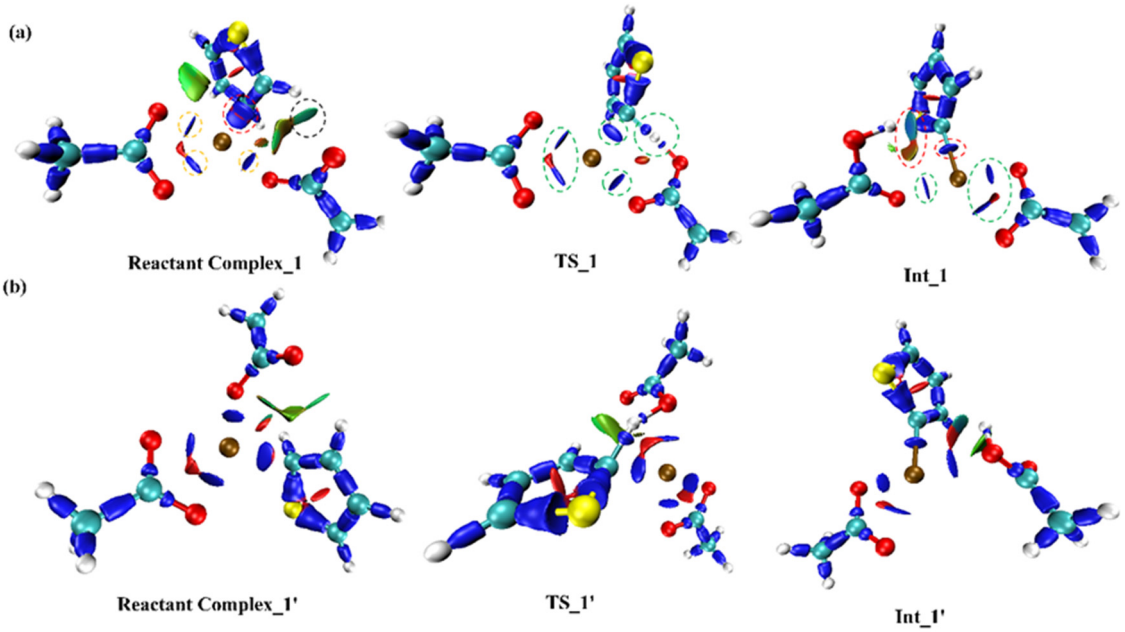

Figure S4. The interaction analysis for each intermediate in C-H activation step for the CMD (a) and σ-metathesis (b) mechanisms.

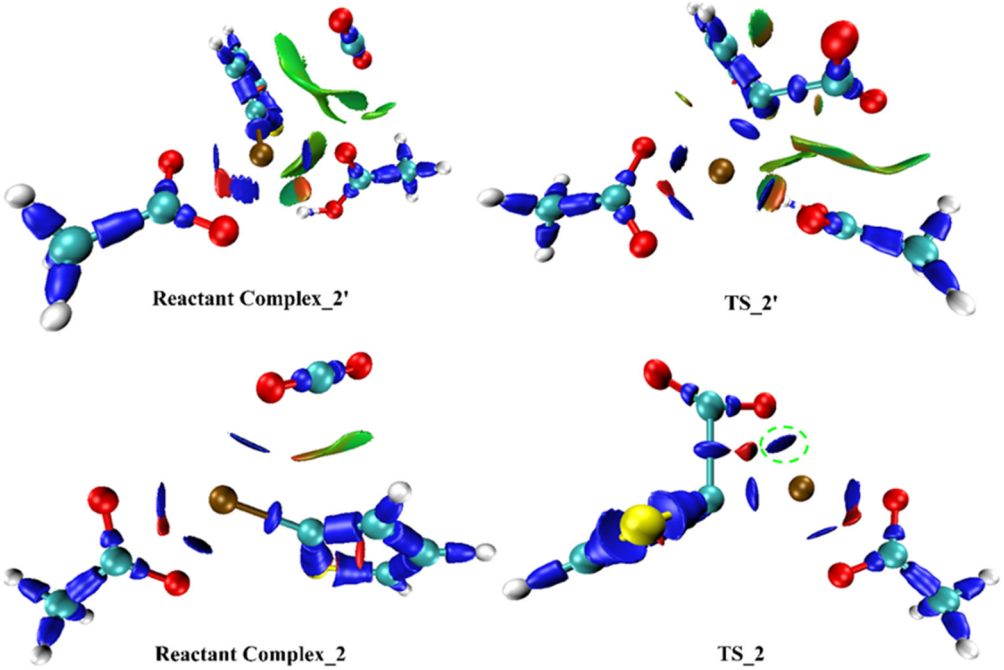

Figure S5. The interaction analysis for each intermediate in CO_2 insertion step.

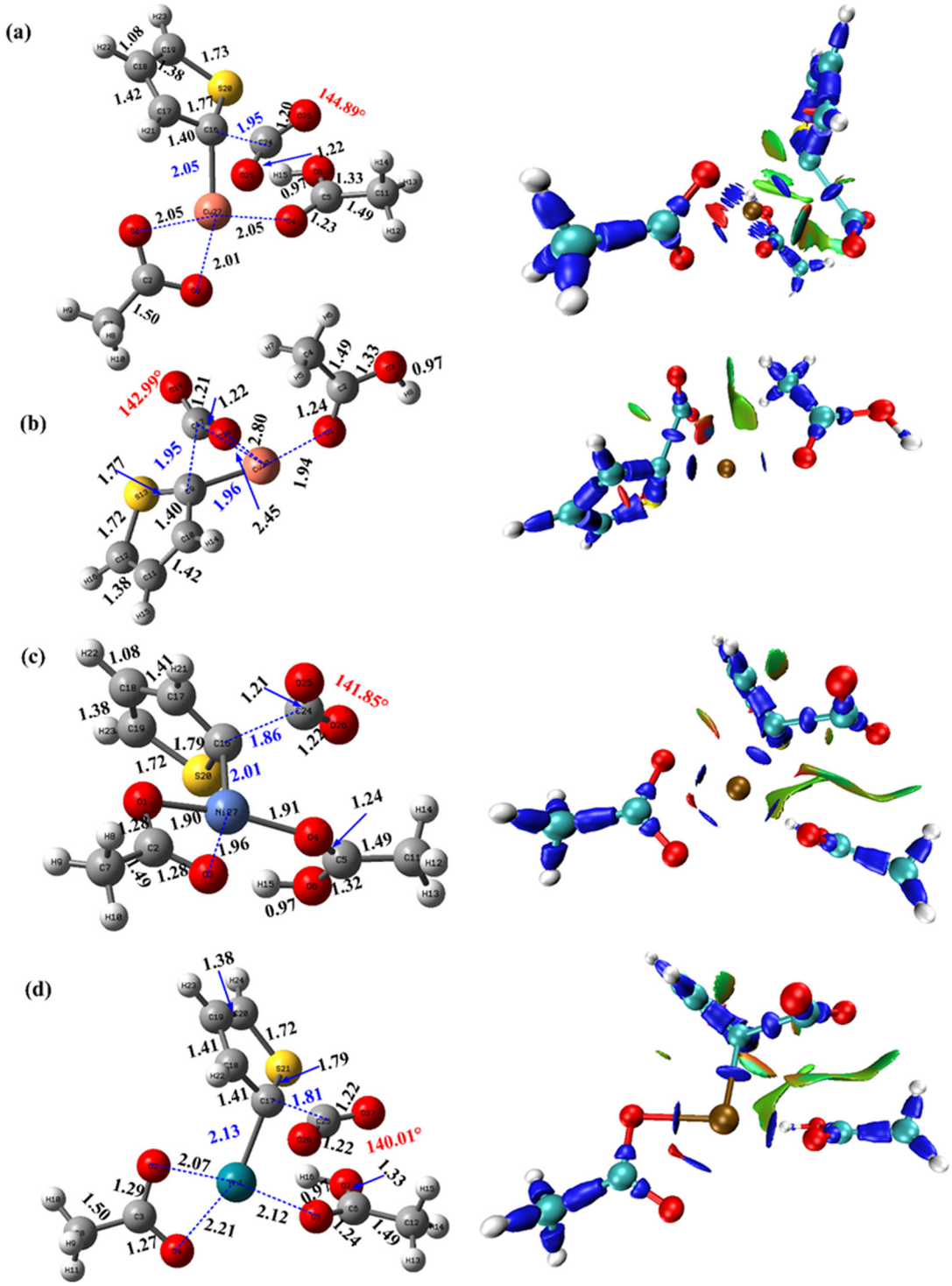

Figure S6. The TS geometry structure and the relevant interaction analyses including acetic acid for CO_2 insertion step: (a) $Cu(OAc)_2$; (b) Cu(OAc); (c) $Ni(OAc)_2$; (d) $Rh(OAc)_2$.

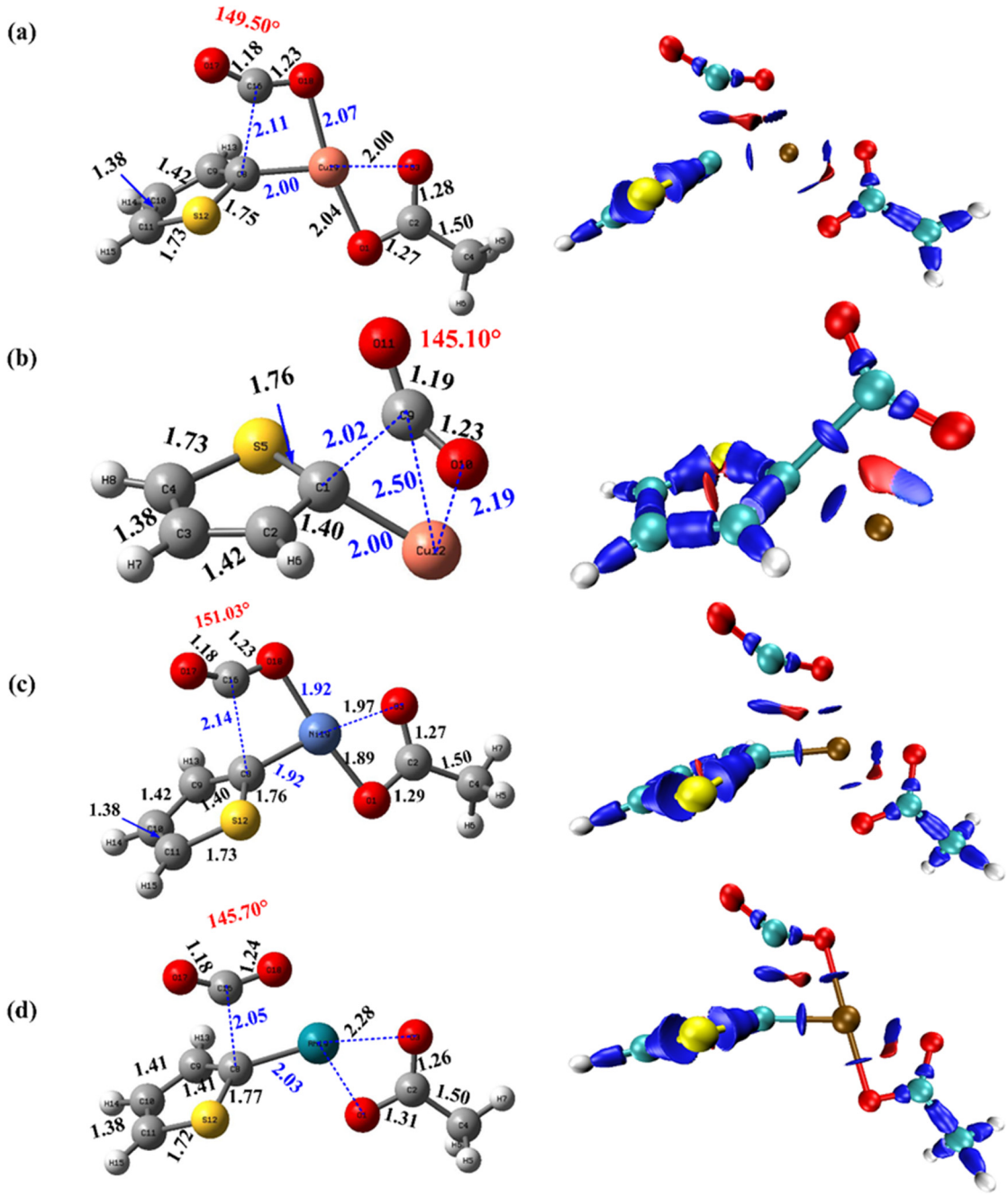

Figure S7. The TS geometry structure and the relevant interaction analyses excluding acetic acid for CO_2 insertion step: (a) $Cu(OAc)_2$; (b) $Cu(OAc)$; (c) $Ni(OAc)_2$; (d) $Rh(OAc)_2$.

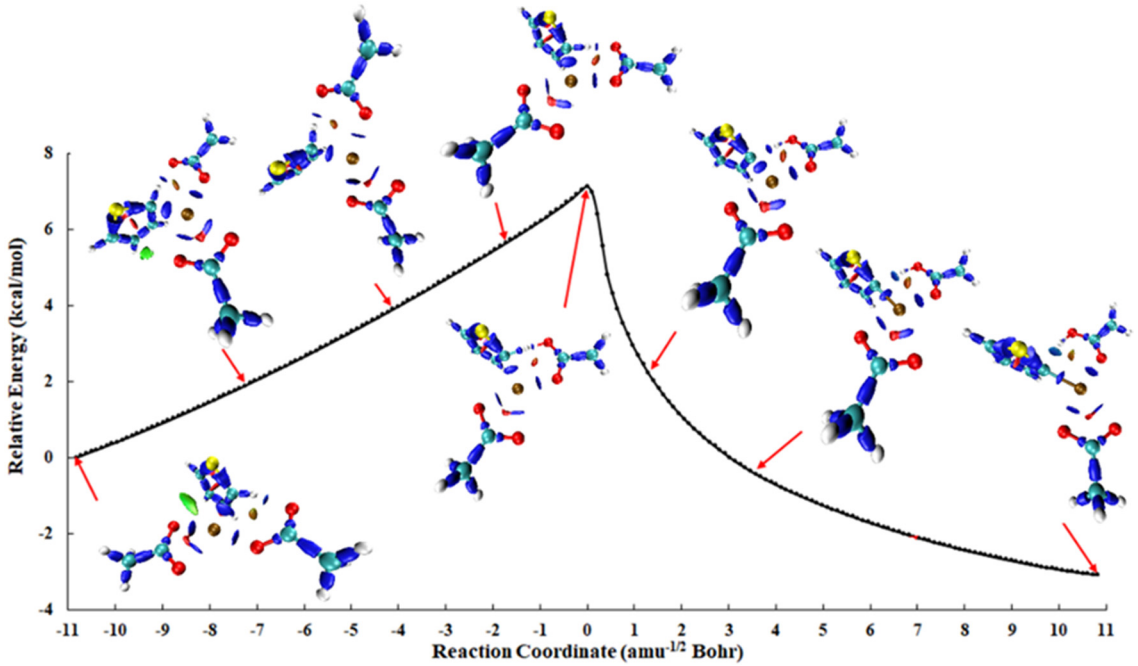

Figure S8. The interaction analysis for thiophene deprotonation step (CMD).

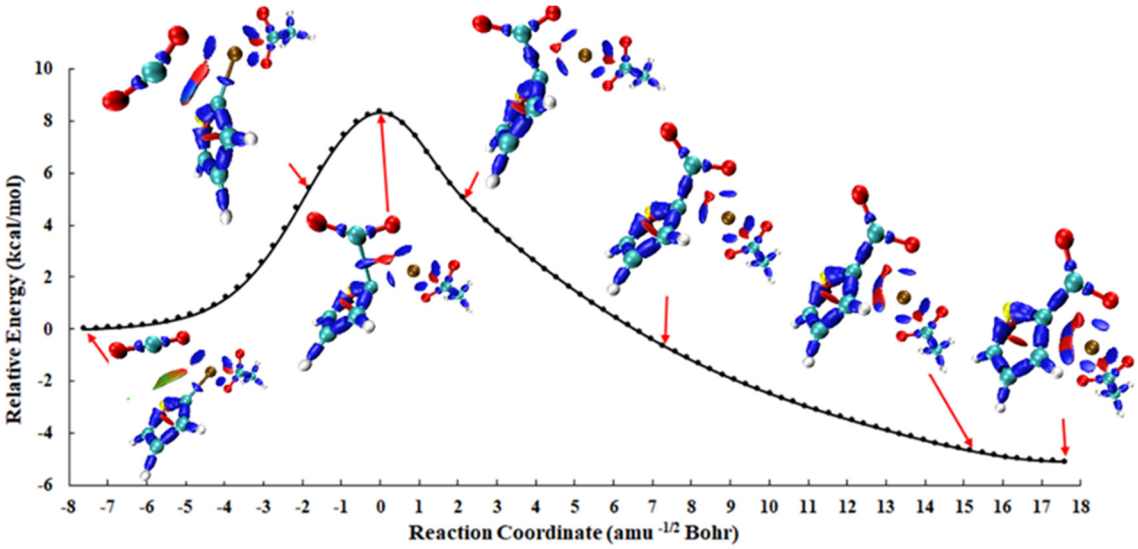

Figure S9. The interaction analysis for the CO_2 insertion step.

References

1. Lu, T.; Chen, Q. Interaction region indicator: A simple real space function clearly revealing both chemical bonds and weak interactions. *Chem. -Methods* **2021**, *1*, 231–239.
2. Lu, T.; Chen, F. Multiwfn: A Multifunctional Wavefunction Analyzer, *J. Comput. Chem.* **2012**, *33*, 580–592.